CELLULOSE NANOCRYSTALS FROM SUGARCANE BAGASSE: ISOLATION, CHARACTERIZATION AND APPLICATION

SICILY RILU JOSEPH, HELEN T. P. SANDRA, ARYA NAIR, SARITHA A. CHANDRAN and MYTHILI USHAMANI

Department of Chemistry and Centre for Research,
St. Teresa's College (Autonomous), Ernakulam, Kerala, India
✉ *Corresponding author: M. Ushamani, ushamanim@teresas.ac.in*

Received September 19, 2022

Sugarcane bagasse (SCB) is a by-product of the sugar industry, with approximately 1.9 billion tonnes produced yearly. The sugar industry produces a huge quantity of bagasse during the manufacture of sugar from sugarcane, which has a negative environmental impact, triggering environmental pollution. In this work, chemically purified cellulose (CPC) and cellulose nanocrystals (CNCs) were very effectively extracted from sugarcane bagasse by the acid-hydrolysis method. The obtained CNCs had a rod-like shape, with a diameter in the range of 2-7 nm, and were used to form a CNC-ZnS nanocomposite. The CNCs were seen to be less agglomerated, and the CNC-ZnS nanocomposite was further tested in an antibacterial study using the agar well diffusion method. The synthesized materials were characterized using a number of analytical techniques. The results demonstrated an enhanced antibacterial property of the CNC-ZnS nanocomposite.

Keywords: chemically purified cellulose, cellulose nanocrystals, sugarcane bagasse, zinc sulphide

INTRODUCTION

Sugarcane bagasse is the remaining fibre residue after sugar extraction and is considered a by-product of the sugar industry. It consists of 45% cellulose, 28% hemicelluloses, 20% lignin, 5% sugar, 1% minerals, and 2% ash. Because of the high moisture content in bagasse, it is used in the manufacture of pulp and paper products, as filler for building materials, as a substrate for growing mushrooms, in ethanol production, and in the preparation of bioplastics. The sugar industry generates huge quantities of bagasse on a global level, and the valorisation of this residue is important to reduce landfill waste and diminish environmental polltion.[1]

Sugarcane bagasse has a high proportion of cellulose, which can be readily isolated by pulping. Bagasse provides an ideal opportunity for producing value-added products from such an inexpensive source of biomass.[2] The extraction of nanocellulose from sugarcane bagasse is easier than that from wood because cellulose microfibrils are organized in a less tightly bound manner in the primary cells of agricultural residue fibers, compared to the secondary walls in wood.

Cellulose, which is the major component in the lignocellulosic biomass of sugarcane bagasse is mainly localised in the plant cell wall in amounts of around 35-50%. It is composed of the linear homopolysaccharide of β-1,4-linked anhydro-D-glucose units with the repeating unit of cellobiose.[3] Other major components are lignin and hemicelluloses, which form the amorphous part of the biomass. Cellulose can be extracted from a variety of plant sources, including wood and non-wood sources, such as hemp, flax, jute, ramie, kenaf, cotton, leaves of sisal and abaca, corncob, risk husk, sugarcane bagasse, apple pomace, grape pomace, passion fruit peels, tea leaf, banana fiber, groundnut shell and plum seed shell.[4] Using agricultural residues or by-products for this purpose brings major economic and environmental benefits.

Nano-dimension cellulose can be of different forms, such as nanocrystals (CNCs) or nanofibrils (CNFs).[5] CNCs are discrete, rod-shaped cellulose nanoparticles, with a high degree of crystallinity and are primarily produced through acid hydrolysis of native cellulose. A strong acid, such

as H_2SO_4 or HCl, is practically used to break the glycoside bond in cellulose. Typically, CNCs contain surface charge groups and have lengths of hundreds to thousands of nanometers. As a result, they can be colloidally stable.[6] CNCs have been found to have numerous applications, which are dependent on their specific morphology and properties, which in turn depend mainly on the original source of cellulose and the extraction methods. The degree of crystallinity and aspect ratio, *i.e.* length to diameter (L/d) ratio, are very important parameters that determine the CNC properties. Aqueous suspensions of CNCs produced by sulfuric acid hydrolysis have been demonstrated to be more stable than those produced by hydrochloric or phosphoric acid hydrolysis. This is due to the introduction of negatively charged sulfate groups on their surface that prevent their agglomeration by electrostatic repulsion.[7]

Traditional plastics causing environmental pollution can be replaced by bio-composites incorporating cellulose nanocrystals. Nanocellulose derived from plant fibres has been extensively used and recommended as a semi-structural fibre replacement in the composite industry. Due to their biodegradability, environmental friendliness, and sustainability, entirely green bio-composites made from nanocellulose have become of great interest.[8,9] The incorporation of CNCs into a polymer matrix, for example, starch, with the addition of glycerol as plasticizer, is expected to yield good mechanical properties.[9] CNCs can be extracted from sugarcane bagasse and composited with potato starch thermoplastic (PST), to develop totally green nanocellulose-based starch thermoplastics, which could replace synthetic plastic-based packaging materials.[10,11]

In recent years, there has been an increasing interest in investigating and developing antimicrobial packaging materials. Nanocellulose-based antimicrobial materials have attracted a great deal of research attention due their many potential applications in various areas, including food packaging, textiles, paints, drug carriers, ultrafiltration, adsorbents and wound dressings.[12] Composites of CNCs with zinc-based nanomaterials have been proved to have significant antibacterial properties.[13]

Our study is based on the extraction of cellulose from sugarcane bagasse and its conversion to cellulose nanocrystals. The raw bagasse, chemically purified cellulose and the cellulose nanocrystals were characterized for surface morphology using transmission electron microscopy (TEM), and Fourier transform infrared spectroscopy (FTIR), and crystallinity analysis using X-ray diffraction (XRD). The CNCs prepared from sugarcane bagasse were then used for preparing nanocomposites with the inclusion of ZnS nanoparticles, and their antibacterial study was performed.

Bacterial infections are a serious health problem that poses a potential threat to human lives and can have serious socio-economic complications. Antimicrobial packaging materials can contribute to diminishing the risks of food-borne bacterial infections, by protecting the food from contamination and prolonging its shelf-life. In our work, we aimed to develop a composite based on ZnS nanoparticles and CNCs with high antibacterial activity. ZnS itself is a material with outstanding antibacterial properties, while cellulose nanocrystals have also been reported to have antibacterial activity, and thus, a synergistic effect of both ZnS and CNCs upon composite formation is expected.

EXPERIMENTAL

Materials

Raw sugarcane bagasse was collected from a local juice shop and used to extract CNCs. Nitric acid (HNO_3), sodium hypochlorite (NaClO), sulfuric acid (H_2SO_4), acetic acid (CH_3COOH), sodium hydroxide (NaOH), zinc chloride (0.1 M), sulphur powder (0.1M), and NaOH (5M) used in the experiments were all of analytical grade.

Preparation

Synthesis of cellulose nanocrystals (CNCs)

Sugarcane bagasse (SCB) was initially washed with distilled water to remove all unwanted impurities. It was then sun-dried and ground into powder using a blender. The powdered bagasse was then oven-dried at 105 °C for about 5 hours. 17.5 g of the bagasse powder was mixed with 250 mL of 6% (w/v) HNO_3 for 2 h in a hot water bath placed at 80 °C, then washed with distilled water until neutral pH was attained. The solution was then refluxed with 200 mL of 1% NaOH at constant stirring for 2 hours at 80 °C in a hot water bath. It was again washed with distilled water and bleached with 200 mL of 5% (w/v) sodium hypochlorite and washed to neutral pH. Acetic acid was further added to the lignocellulosic extract and stirred for 2 h at 80 °C. The residue was then washed with deionized water until neutral pH and left to dry at room temperature to obtain cellulose.

CNCs were prepared from the isolated cellulose. Chemically purified cellulose from SCB was

hydrolyzed with 32% H_2SO_4 at a 1:25 g/mL ratio at 60 °C for 5 h with constant stirring. This reaction was then quenched by the addition of 10-fold deionized water to the reaction mixture, followed by centrifugation at 4000 rpm for 30 min to remove the acidic solution till neutral. A highly stable colloidal suspension was obtained, which was then sonicated for 2 hours to homogenise the generated cellulose nanocrystals. The generated nanocrystals were further centrifuged at 4000 rpm for 30 min. The colloidal suspension of cellulose nanocrystals (CNCs) was stored at 4 °C in a refrigerator until further use.[1]

Synthesis of zinc sulphide nanoparticles in alkaline medium

Zinc chloride (0.1M) and sulphur powder (0.1M) were separately dissolved in distilled water and made up to 100 mL, and then mixed with a magnetic stirrer at 70 °C. NaOH (5M) was slowly added into the mixture until an alkaline pH was attained. It was then kept for 5 hours under constant stirring. The precipitate was washed several times with distilled water and centrifuged at 6000 rpm for 10 minutes. The sample was then dried in the oven at 80 °C for 2 hours and annealed at 300 °C to obtain ZnS nanoparticles.[14]

Synthesis of ZnS-CNC composite materials

Zinc chloride (0.1M) and sulphur powder (0.1M) were separately dissolved in distilled water and made up to 100 mL, and then mixed with a magnetic stirrer at 70 °C. CNCs (1 g) dissolved in 100 mL of water was added to this mixture. NaOH was added slowly to the mixture until an alkaline pH of 10.44 was attained. It was then kept for 5 hours with constant stirring. The precipitate obtained was washed, filtered and dried at 50 °C.[15]

Scheme 1 shows the various stages of preparation and the obtained products.

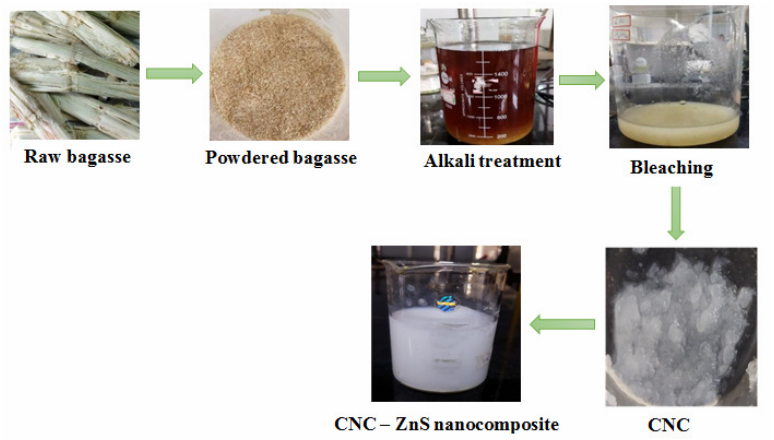

Scheme 1: Procedure for the preparation of CNC-ZnS

Antimicrobial assay by agar well diffusion method

The antibacterial activities of the CNCs, ZnS and CNC-ZnS were assessed by the agar well diffusion method. 1 ml of a fresh culture of *E. coli* was inoculated on sterile Petri dishes. Wells were made using a sterile cork borer into the agar plates containing inoculum. Then, 100 µL of each test solution was added to respective wells. The test solutions were CNC, ZnS and the CNC-ZnS nanocomposite. Then, the plates were incubated at 37 °C for 24 hours. Antimicrobial activity was detected by measuring the zone of inhibition (including the diameter of the wells) that appeared after the incubation period. Distilled water was employed as a negative control. Tetracycline antibiotic was used as a standard.

Characterization

The changes in the functional groups of the materials SCB, CPC and CNCs were investigated by FTIR spectroscopy using a Nicolet iS50 FTIR spectrophotometer. The FTIR spectra of the samples were recorded in the transmittance mode, in the range from 4000 cm^{-1} to 100 cm^{-1}.

The crystallinity index of the SCB before and after chemical modification was analysed using a Bruker D8 Advance X-ray Diffractometer. SCB, CPC and CNCs in the form of powder were placed on steel sample holders and levelled to obtain total and uniform X-ray exposure. The samples were analyzed at 25 °C, with a monochromatic CuKα radiation source λ = 0.1539 nm with a 2 theta angle ranging from 10° to 60°. The crystallinity index was calculated as:

$$C_rI(\%) = \frac{I002 - Iam}{I002} \times 100 \quad (1)$$

where I_{002} denotes the maximum intensity of the I_{002} lattice diffraction peak and I_{am} is the minimum intensity scattered by the amorphous part of the sample.

Morphological properties and particle sizes of CNCs were determined using a Jeol/JEM 2100 Transmission Electron Microscope. The samples were

dispersed in a suitable medium and then placed on a copper grid coated with a carbon film.[1]

SEM, EDAX and XRD techniques were used to characterize the prepared ZnS nanoparticles. The prepared ZnS samples were analyzed by X-ray powder diffraction (XRD) using a Bruker D8 Advance X-ray Diffractometer, with a Cu-Kα radiation source of 0.1539 nm wavelength, in the range of 10°–90° of Bragg's angle, to determine the structural parameters. A scanning electron microscope (SEM) (Model: Joel 6390LA) with an image analyzer was used to analyze the morphological features of ZnS. EDAX can be employed to identify the elemental composition of the ZnS sample.[16]

RESULTS AND DISCUSSION

Characterization of cellulose materials

Physical appearance

The physical appearance of the raw sugarcane bagasse, powdered bagasse, chemically purified cellulose and its nanocrystals prepared by the hydrolysis method is shown in Figure 1. The raw sugarcane bagasse and its powdered form had a brown color, but it was whitened as a result of the chemical treatment. The treatment of the bagasse with HNO_3, NaOH and sodium hypochlorite also changed the texture of the powder. The hydrolysis of the extracted cellulose with H_2SO_4 acid produced the nanocrystals that were whiter and finer in texture.

Fourier transform infrared (FTIR) spectroscopy analysis

Structural changes of the SCB were determined by FTIR, which was performed before and after chemical treatment. The infrared spectra of SCB, CPC and CNCs are shown in Figure 2. The broad peak at 3100-3500 cm^{-1} indicates the O–H stretching bonds, while the peak around 2800-2950 cm^{-1} indicates the C–H stretching. The peak around 1750 cm^{-1} corresponds to the C–O bond, which is normally found in the linkages of the esters in the hemicelluloses and lignin. The peaks observed around 1600-1700 cm^{-1} indicates the aromatic ring found in the lignin. The peak between 1200-1300 cm^{-1} depicts an out of plane C–O stretching in the aryl group of the lignin present in the SCB before chemical modification. The modification of SCB with sodium chloride and sodium hypochlorite led to the disappearance of these bands – as can be seen in the FTIR spectra of CPC and CNCs (Fig. 2). The outcome of this chemical treatment can be noted from the main spectral bands between 1500-1600 cm^{-1} and around 1250 cm^{-1}. The two spectral bands at these positions are seen to disappear after the chemical treatments performed to obtain the CPC and CNCs. The FTIR spectrum of CNCs is similar to that of CPC, but it has sharper bands. The peaks observed at 1600-1650 cm^{-1} for the CPC and CNCs are the result of O–H bending due to adsorbed water, the bands between 1400-1450 cm^{-1} are attributed to CH_2 intertwined in the cellulosic material. The peak at 1050 cm^{-1} indicates the C–O–C pyranose ring stretching vibration. The peak observed around 900 cm^{-1} is reported to be associated with the cellulosic β-glycosidic linkages. These results depict the formation of cellulose nanocrystals.

X-ray diffraction (XRD) analysis

The X-ray diffraction patterns of SCB, CPC and CNCs are shown in Figure 3. The crystallinity index of SCB, CPC and CNCs was calculated from the XRD. The crystallinity index (CrI) denotes the ratio of the crystalline constituents to the amorphous regions of a material. The SCB, CPC and CNCs exhibited three main characteristic peaks around 2θ of 16°, 22.1° and 34.7°. The peaks represent the characteristic patterns for the crystal form of cellulose I polymorph, since there is no doublet peak around 2θ value of 22°. The peak at 2θ of 16° corresponds to the (110) crystallographic plane, while those at 2θ of 22.1° and 34.7° are related to the (002) and (004) crystallographic planes, respectively. After the treatment, more intense crystalline peaks were observed with the main reflections at 2θ of 22.1° and 34.7°. This was also a confirmation of the successful removal of the lignin from the bagasse. The high peak intensity around 2θ of 22.1° is correlated to the crystalline structure of cellulose. Also, from the XRD patterns, the presence of a broad peak around 2θ of 16° is characteristic of an amorphous arrangement.

The crystallinity index (CrI) of SCB, CPC and CNCs, calculated for the XRD patterns, presented an increase in crystallinity in the following order: SCB < CPC < CNCs. The crystallinity indices of SCB and CNCs were 27.1905% and 67.1574%, respectively. From the experimental data, SCB presented the lowest CrI, due to its higher amounts of amorphous constituents. After chemical treatment using sodium hydroxide and sodium hypochlorite in the extraction of the cellulose, crystallinity increased.

This is attributed to successful elimination of hemicelluloses and lignin that were attached to

the cellulosic bagasse. The crystallinity index was also observed to further increase in CNCs after acid hydrolysis using sulfuric acid. The increase in crystallinity upon acid hydrolysis depicted the dissolution of the amorphous region of the SCB. During the chemical treatment, sulfuric acid reacts with the amorphous region of SCB, causing hydrolytic cleavage of the glycosidic bonds, thus releasing individual crystallites. This, in turn, causes the growth of monocrystals, which contributes to the increase in crystallinity, which is observed as narrow and pronounced diffraction peaks in the XRD pattern.

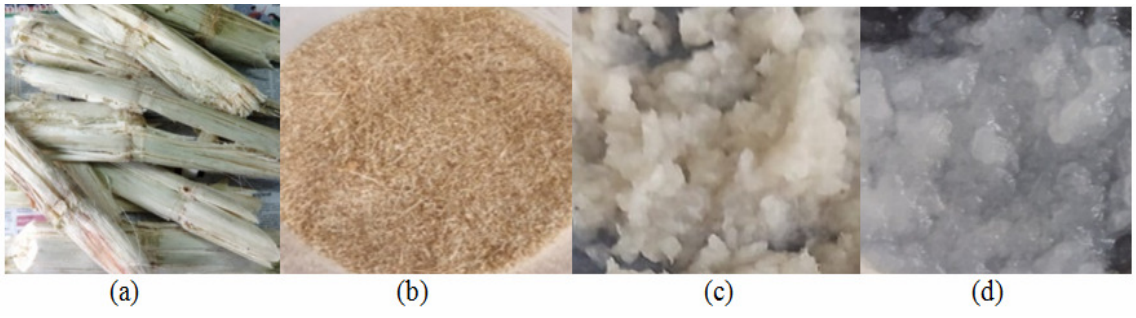

Figure 1: Photographs showing raw materials, intermediate and final product: sugarcane bagasse (a), crushed sugarcane bagasse (b), extracted cellulose (c) and cellulose nanocrystals (d)

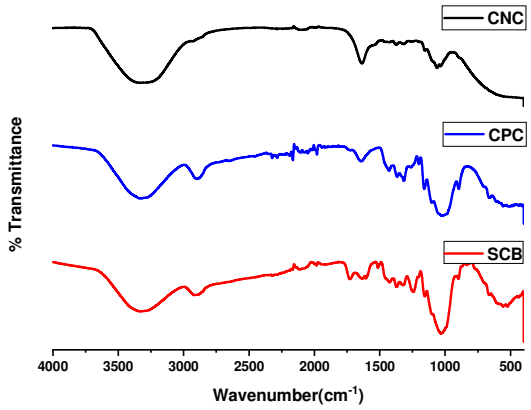

Figure 2: FTIR spectra of sugarcane bagasse (SCB), chemically purified cellulose (CPC) and cellulose nanocrystals (CNC)

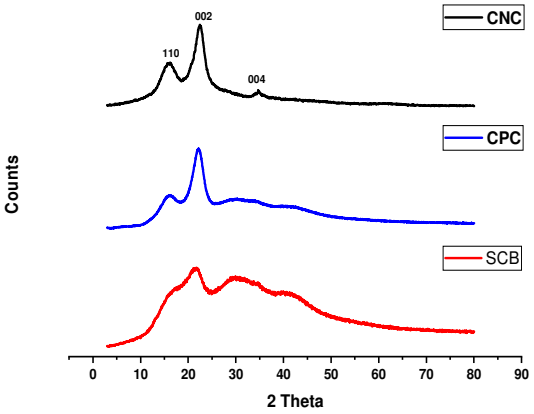

Figure 3: X-ray diffraction patterns of sugarcane bagasse (SCB), chemically purified cellulose (CPC) and cellulose nanocrystals (CNC)

Transmission electron microscopy (TEM)

Transmission Electron microscopy was used to study the morphology and determine the particle size of the cellulose nanocrystals (Fig. 4). The chemical treatment of the SCB with an alkali solution and further by acid hydrolysis was expected to remove the hemicelluloses and lignin, which form the amorphous region of the cellulosic bagasse. Acid hydrolysis is aimed at reducing the size of the cellulose to the nanometer range, while leaving the crystalline regions intact.

As can be seen in Figure 4 (a), the CNCs have a 'rod-like' shape, with an average diameter of 2-7 nm. A few agglomerations are observed, which can be attributed to the presence of strong hydrogen bonds within the CNCs, indicating their hydrophilic nature. The corresponding SAED pattern illustrates a series of bright spots, which are due to the diffraction from the crystallites of nanocrystals. This indicates a highly crystalline nature of the synthesized CNCs.

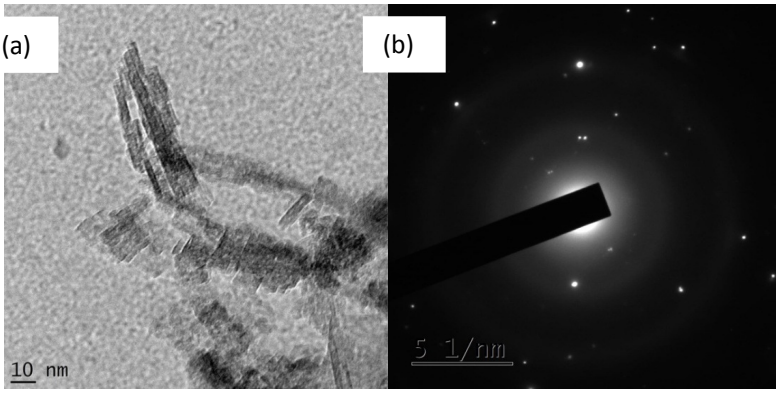

Figure 4: (a) TEM image and (b) SAED image of cellulose nanocrystals

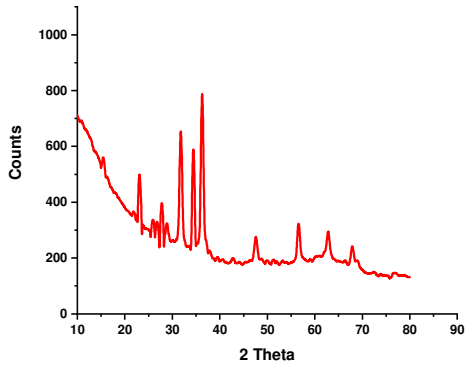

Figure 5: XRD pattern of synthesized zinc sulphide nanoparticles in alkaline medium

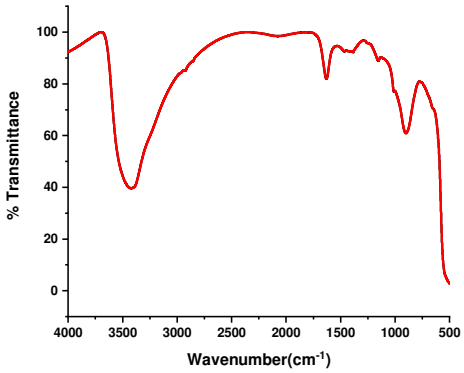

Figure 6: FT-IR spectrum of synthesized zinc sulphide nanoparticles in alkaline medium

Characterization of zinc sulphide (ZnS) nanoparticles

The crystal size of ZnS nanoparticles was analyzed by XRD studies. Figure 5 shows the XRD pattern of zinc sulphide nanoparticles synthesized in alkaline medium. The pattern reveals three clear peaks. The average crystal size was determined using the Debye Scherrer equation: $D = 0.9\ \lambda/B\ \cos\theta$. The average crystal size was found to be 41.2402 nm. This confirms that the particles belong to the nano-size range.

FT-IR analysis was performed in order to determine the functional groups of the synthesized ZnS nanoparticles in alkaline medium. The FTIR spectrum of ZnS nanoparticles is presented in Figure 6, and reveals the chemical bonding between zinc and sulphur. The broad absorption bands at 3423.59 cm^{-1} and 1629.96 cm^{-1} are attributed to O-H stretching and bending vibrations of the absorbed water molecules on the surface of nanoparticles. The peak appearing at 432.95 cm^{-1} is associated to ZnS vibration and is characteristic of cubic ZnS. The metal to sulphur bond formation is confirmed by the peak at 1384.28 cm^{-1}, which can be attributed to carboxyl groups (C=O), also showing a characteristic band at 1153.06 cm^{-1}.

SEM was conducted in order to examine the morphology of ZnS nanoparticles. The SEM image shown in Figure 7 reveals that the synthesized ZnS particles had grain morphology. EDAX was also performed in order to determine the elemental composition of the samples. Figure 8 presents the EDAX spectrum of synthesized ZnS nanoparticles. The spectrum reveals the presence of two major elements, which are zinc and sulphur. The presence of oxygen is due to the oxidation of ZnS to ZnO, while annealing at high temperatures.

Antimicrobial studies

The antibacterial activity of the prepared CNC-ZnS nanocomposite was observed against *Escherichia coli* (gram-negative), along with that of the synthesized cellulose nanocrystals, and ZnS (Fig. 9). The antibacterial activity was determined by measuring the diameter of the inhibition zone formed around the wells on the plate.

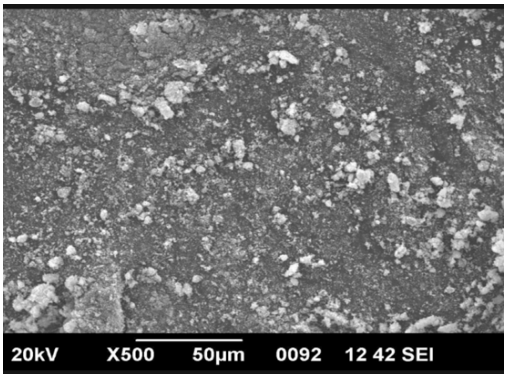

Figure 7: SEM image of synthesized zinc sulphide nanoparticles in alkaline medium

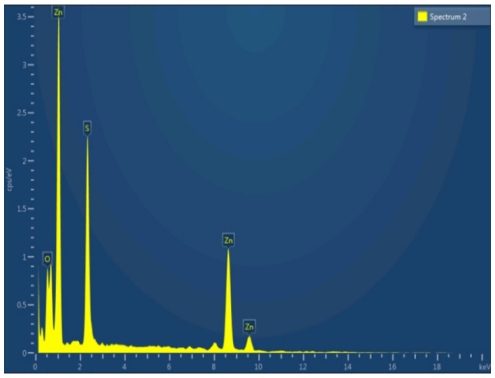

Figure 8: EDAX spectrum of synthesized zinc sulphide nanoparticles in alkaline medium

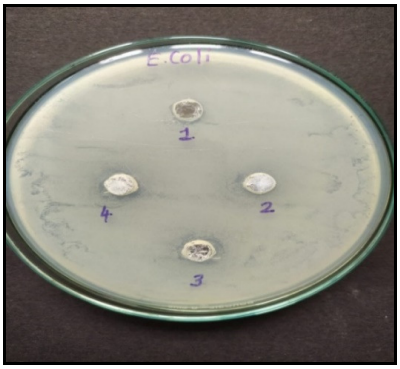

Figure 9: Antibacterial activity of synthesized cellulose nanocrystals, ZnS, CNC-ZnS composite and Tetracycline against *Escherichia coli*

Table 1
Diameter of inhibition zone for CNCs, ZnS, CNC-ZnS and Tetracycline against *E. coli*

Sample	Diameter of inhibition zone
CNC	0.8 cm
ZnS	1 cm
ZnS-CNC	1.1 cm
Tetracycline	1.2 cm

After incubation for 24 hours, it was found that CNCs have a small bacteriostatic effect against *E. coli*, showing an inhibition zone with the diameter of 0.8 cm. As expected, ZnS showed higher inhibition of bacterial growth. Meanwhile, the combination of cellulose nanocrystals and ZnS made possible a synergistic effect of the components, which led to an enhancement in antibacterial activity, with an increase in the diameter of the inhibition zone to 1.1 cm (Table 1).

These results are confirmed by previous studies, where nanocomposites formed via the incorporation of zinc nanoparticles into cellulose based substrates have reportedly shown enhanced antibacterial activity, compared to their individual components. For example, M. El-Sakhawy *et al.*[17] achieved an enhancement in antibacterial activity against *E. coli* from 0.9 cm to 2.3 cm by incorporating ZnO nanoparticles into TEMPO-cellulose nanofibre (CNF). The inhibition of bacterial growth obtained for the composite was comparable with that of Ampicillin used as standard. D. Pathania *et al.*[18] have also done similar work against *E. coli*, wherein the ZnS-cellulose nanocomposite showed a zone of inhibition of 1.2 cm at an optimum concentration of 2 mg/mL. However, this result was very low, compared to the inhibition zone of 2.2 cm obtained by Tetracycline under similar conditions. In our current study, Tetracycline showed an inhibition zone with the diameter of 1.2 cm,

which is close to that achieved by the nanocomposite under similar conditions, at a concentration of 5 mg/mL. The isolated nanocellulose can be considered an appropriate reinforcement to develop polymeric composites for antibacterial packaging applications.[19,20]

CONCLUSION

This study aimed to demonstrate the viability of the preparation of CNCs from sugarcane bagasse, which is a by-product of the sugar industry and can turn into an environmental threat if not valorized properly, and to further develop a low-cost antibacterial agent via composite formation with CNCs and ZnS nanoparticles. A stable suspension of rod-shaped nanocrystalline cellulose, with the diameter in the range of 2-7 nm, was developed via acid hydrolysis. Prior to acid hydrolysis, bleaching of biomass was performed to remove as much of the non-crystalline and non-cellulosic components of biomass as possible. This aids in reducing hydrolysis time and producing CNCs of uniform dimensions. An increase in crystallinity was observed for the nanocrystals by XRD, which indicated the exposure of the crystalline phase after successful elimination of the lignin and hemicelluloses. FTIR analysis showed the disappearance of the peaks corresponding to hemicelluloses and lignin after the pretreatment, confirming their elimination. The particle size was greatly reduced in diameter after the acid hydrolysis of cellulose, as observed by TEM, and this is an indicator of improved properties of the CNCs. The SAED pattern shows a series of bright spots due to the diffraction from the crystallites of nanocrystals, indicating the highly crystalline nature of the synthesized CNCs.

The antibacterial properties of the CNCs incorporated with ZnS nanoparticles were studied. The antimicrobial activity of the CNCs, ZnS and ZnS-CNC composite was evaluated against *Escherichia coli*. The study reveals an enhancement in the antibacterial activity of the ZnS-CNC composite, which is comparable to that of the antibiotic. The prepared ZnS-CNC composite will be further investigated for the development antibacterial packaging materials.

REFERENCES

[1] S. K. Evans, O. N. Wesley, O. Nathan and M. J. Moloto, *Heliyon*, **5**, 2405 (2019), https://doi.org/10.1016/j.heliyon.2019.e02635

[2] D. Bhattacharya, L. T. Germinario and W. T. Winter, *Carbohyd. Polym.*, **73**, 371 (2008), http://dx.doi.org/10.1016/j.carbpol.2007.12.005

[3] K. Gajanana and S. N. Tijareb, *Mater. Today Procs.*, **5**, 1093 (2018), https://doi.org/10.1016/j.matpr.2017.11.187

[4] H.-M. Ng, L. T. Sin, T.-T. Tee, S.-T. Bee, D. Hui *et al.*, *Compos. B: Eng.*, **75**, 176 (2015), https://doi.org/10.1016/j.compositesb.2015.01.008

[5] R. E. Abou-Zeid, R. Khiari, N. El-Wakil and A. Dufresne, *Biomacromolecules*, **20**, 573 (2018), https://doi.org/10.1021/acs.biomac.8b00839

[6] W. T. Wulandari, A. Rochliadi and M. Arcana, *IOP Conf. Series: Mater. Sci. Eng.,* **107**, 012045 (2016), https://iopscience.iop.org/article/10.1088/1757-899X/107/1/012045/pdf

[7] Kusmono, R. F. Listyanda, M. W. Wildan and M. N. Ilman, *Heliyon*, **6**, e05486 (2020), https://doi.org/10.1016/j.heliyon.2020.e05486

[8] P. Balakrishnan, M. S. Sreekala, M. Kunaver, M. Huskic and S. Thomas, *Carbohyd. Polym.*, **169**, 176 (2017), https://doi.org/10.1016/B978-0-12-820352-1.00074-2

[9] E. Tavassoli-Kafrani, M. V. Gamage, L. F. Dumee, L. Kong and S. Zhao, *Crit. Rev. Food Sci. Nutr.*, **62**, 2432 (2022), https://doi.org/10.1080/10408398.2020.1853038

[10] P. Balakrishnan, S. Gopi, M. S. Sreekala and S. Thomas, *Starch/Staerke*, **70**, 1 (2018), https://doi.org/10.1002/star.201700139

[11] D. C. D. Midhun, R. Derval dos Santos, P. H. Camani, A. S. Kumar, K. V. Neenu *et al.*, *Int. J. Biol. Macromol.*, **191**, 572 (2021), https://doi.org/10.1016/j.ijbiomac.2021.09.103

[12] M. N. F. Norrrahim, N. M. Nurazzi, M. A. Jenol, M. A. A. Farid, N. Janudin *et al.*, *Mater. Adv.*, **2**, 3538 (2021), https://doi.org/10.1039/D1MA00116G

[13] M. Balouiri, M. Sadiki and S. Koraichi Ibnsouda, *J. Pharmaceut. Anal.*, **6**, 71 (2016), https://doi.org/10.1016/j.jpha.2015.11.005

[14] B. Sreenivasulu, B. Rama Sagar, S. Venkatramana Reddy and B. Sankara Reddy, *Ferroelectrics*, **577**, 91 (2021), https://doi.org/10.1080/00150193.2021.1916353

[15] D. Pathania, M. Kumar and V. Kumar Gupta, *Mater. Design*, **87**, 1056 (2015), https://doi.org/10.1016/j.matdes.2015.08.103

[16] S. Sagadevan and P. Koteeswari, *J. Nanomed. Res.*, **2**, 48 (2015), https://doi.org/10.15406/jnmr.2015.02.00040

[17] M. El-Sakhawy, A. Salama, A. K. El-Ziaty and H. Hassan, *Cellulose Chem. Technol.*, **55**, 365 (2021), https://doi.org/10.35812/CelluloseChemTechnol.2021.55.35

[18] D. Pathania, M. Kumari and V. Kumar Gupta, *Mater. Design*, **87**, 1056 (2015), https://doi.org/10.1016/j.matdes.2015.08.103
[19] N. Raval, R. Maheshwari, D. Kalyane, S. R. Youngren-Ortiz, M. Chougule *et al*., in "Basic Fundamentals of Drug Delivery", edited by R. K. Tekade, Academic Press, 2019 pp. 369-400, http://dx.doi.org/10.1016/B978-0-12-817909-3.00010-8
[20] D. A. Gopakumar, S. Thomas and Y. Grohens in "Multifunctional Polymeric Nabocomposites Based on Cellulosic Reinforcements", edited by D. Puglia, E. Fortunati and J. M. Kenny, Elsevier, 2016, pp. 253-272, https://doi.org/10.1016/C2014-0-04565-0